

Available online at [www.sciencedirect.com](http://www.sciencedirect.com)

ScienceDirect

journal homepage: [www.elsevier.com/locate/jasi](http://www.elsevier.com/locate/jasi)

## Original Article

# Changing population of neurons and glia in the human cochlear nucleus with progressive age – A stereological study

S. Sharma <sup>a</sup>, T.C. Nag <sup>b</sup>, D.N. Bhardwaj <sup>c</sup>, Perumal Vanamail <sup>d</sup>, T.S. Roy <sup>e,\*</sup><sup>a</sup> Assistant Professor, Department of Anatomy, Vardhaman Mahavir Medical College and Safdarjung Hospital, New Delhi 110029, India<sup>b</sup> Professor, Department of Anatomy, All India Institute of Medical Sciences, New Delhi 110029, India<sup>c</sup> Professor, Department of Forensic Medicine, All India Institute of Medical Sciences, New Delhi 110029, India<sup>d</sup> Assistant Professor, Department of Obstetrics and Gynaecology, All India Institute of Medical Sciences, New Delhi 110029, India<sup>e</sup> Professor and Head, Department of Anatomy, All India Institute of Medical Sciences, New Delhi 110029, India

## ARTICLE INFO

## Article history:

Received 20 October 2014

Accepted 6 November 2014

Available online 26 November 2014

## Keywords:

Human auditory nucleus

Morphometry

Aging changes

Stereology

Cluster analysis

## ABSTRACT

**Introduction:** The human cochlear nucleus (CN) is populated by morphologically diverse types of neurons that contribute specifically in the formation of the complex functional networks in the auditory pathway. On the basis of cytoarchitecture and topography different types of neurons can be identified in the CN. The present study was undertaken to investigate the morphological parameters of neurons and glia of the human CN with aging. **Methods:** Forty-one brainstems (Birth–90 years) from cadaveric donors were collected from the mortuary of the All India Institute of Medical Sciences (AIIMS), New Delhi, with ethical committee permission. They were grouped into nine decades and processed for light microscopy and morphometry. Hierarchical clustering was done to classify the neuron population according to their neuronal and nuclear area into different clusters.

**Results:** There was a gradual increase in the mean neuronal and neuronal nucleus volume from decade 1 to 3. Decade 1 had minimum and 3 had maximum nuclear volume and neuron number respectively. An increase in total glial population was observed in decade 9. Eight neuron clusters were identified which were present in the decades 2 and 3 whereas decades 1 and 4 had seven, decades 5–8 had six and decade 9 had four clusters respectively. **Discussion:** Major changes were observed within the clusters from middle to old age, especially after decade 5. This may be useful in explaining the vulnerability of some specific subpopulation of neurons more than others and understanding the pathophysiology of altered hearing loss with age.

Copyright © 2014, Anatomical Society of India. Published by Reed Elsevier India Pvt. Ltd. All rights reserved.

\* Corresponding author. Tel.: +91 11 26594880, 26593216; fax: +91 11 26588663.

E-mail addresses: [tarasankar@hotmail.com](mailto:tarasankar@hotmail.com), [tsroy@aiims.ac.in](mailto:tsroy@aiims.ac.in) (T.S. Roy).

<http://dx.doi.org/10.1016/j.jasi.2014.11.002>

0003-2778/Copyright © 2014, Anatomical Society of India. Published by Reed Elsevier India Pvt. Ltd. All rights reserved.

## 1. Introduction

Altered hearing is a common problem and the degree of impairment and its prevalence increases with age.<sup>1</sup> Age related hearing loss (presbycusis) affects two critical aspects of hearing; it reduces the threshold sensitivity and the ability to understand speech. The loss in hearing threshold sensitivity is insidious in onset, involving initially the highest frequencies, which then slowly progresses and manifests clinically in the fifth to sixth decades.<sup>2</sup> It further leads to difficulty in understanding speech, especially in a noisy environment, which has a major impact on the social and emotional health of the elderly.<sup>3–5</sup> Electrophysiological studies suggested that the alterations in the physiological responses in the aging auditory system correspond with the described morphological changes.<sup>6</sup>

The human cochlear nucleus (CN) is the first relay station in the central auditory pathway and is located at the pontomedullary junction of the brainstem. The auditory nerve enters the CN, bifurcates and sends branches to the ventral and dorsal cochlear nuclei (VCN and DCN). Although there are indistinct boundaries between the two subdivisions in the human CN, different types of neurons can be identified on the basis of their shape, size and location.<sup>7–9</sup> The neurons of the CN receive their input from the type I and type II auditory nerve fibres arising from respective types of spiral ganglion cells (SGC) innervating the inner and outer hair cells of the organ of Corti (cochlea), respectively in the peripheral auditory pathway.<sup>10</sup> Type I fibres innervate all parts except the granule cell layer of the CN that receives type II auditory nerve fibres.<sup>10</sup> Numerous studies have reported that the decline of peripheral auditory input lead to series of degenerative changes in the hair cells, SGC and its axons that result in reduced number of cochlear nerve endings on CN neurons.<sup>11–13</sup>

Available data on the morphology of the human CN with or without history of hearing loss are confusing.<sup>14–17</sup> Studies using various methodologies have documented changes in the neuron number, volume and the size of the CN with age. However, little information is available on age related changes in glial cells in the CN.<sup>18,19</sup> Glial cells are one of the major cell populations of the central nervous system (CNS) and responsible guidance and support of neuronal migration during development, maintenance of the neural microenvironment and immune system.<sup>20,21</sup> Therefore, in the current study we have investigated the human CN morphology from birth to 90 years of age using stereological morphometric methods to get reliable, consistent and reproducible data.<sup>22</sup> Further, the entire neuronal population was classified according to neuron and its nuclear size into different clusters. In the CN, the total neuron and glial numbers and the volume and area of the neurons, their nuclei and the entire CN were measured in all ages and changes were observed within all neuron clusters.

## 2. Materials and methods

### 2.1. Brainstem collection and tissue preparation

Forty-one brainstems were collected from human cadavers, aged between 2 days and 90 years between 2008 and 2012 from

the mortuary of All India Institute of Medical Sciences (AIIMS) in accordance with the protocol approved by the Ethics Committee (Ref. No. E Sub-C/A-20/2.08.2008), AIIMS, New Delhi, India, following the guidelines of Helsinki declaration. Brain samples were obtained using strict exclusion criteria<sup>19</sup> and were grouped into nine decades according to their biological age: birth – 10 years (decade 1), 11–20 years (decade 2) etc. until decade 9.<sup>19</sup> All decades except the first and ninth had five samples each. The first decade had four samples; whereas the ninth had two samples. All specimens were obtained within 6–12 h of death, immersion fixed in 4% paraformaldehyde in 0.1 M phosphate buffer (PB, pH 7.4) and preserved at 4 °C in a refrigerator. No post-mortem changes were observed in all cases studied as confirmed under light microscopy.

The total brain weight was measured in all cases studied. The portion of the brainstem with CN and cochlear nerve was excised and sectioned in two sagittal halves by a midline incision. Both the tissue blocks (right and left half) were kept in the fixative for 1–2 weeks at 4 °C. A tissue block, with the CN, measuring approximately 15 mm in length, was obtained from the brainstem. In all samples, the CN area was chosen for processing. The tissue blocks were washed in 0.1 M PB (pH 7.4) and cryoprotected in 30% sucrose. The caudal end (medullary side) was kept as the cutting surface. For morphometry, stereology was planned as done in our previous studies.<sup>23,24</sup> For stereology, serial transverse, 40 µm thick sections of the CN were cut in a caudal-to-rostral direction (medulla to pons), using a cryotome (Microm International GmbH, Germany), and retrieved approximately 120 sections per sample. The extent of the CN and its neurons were identified and the CN neurons were differentiated from adjacent other neuronal bodies<sup>7,9,19</sup> by using Luxol fast blue stained sections.<sup>19</sup> Glial cells were distinguished from small neurons based on their morphological appearance.<sup>25</sup> After establishing the study design (detail description in next section) every 12th section of the tissue block containing CN was stained with 1% cresyl violet acetate (CV), mounted with DPX and examined under an Olympus BX26 research microscope (Japan). The morphology of the CN viewed with the luxol fast staining was corroborated with CV stained sections. Approximately total twelve CV stained sections per tissue sample were used for stereology.

### 2.2. Stereological estimates

The cresyl violet stained sections of the CN were studied using the Olympus BX26 research microscope attached to a motorized stage controller (LUDL, Germany) and a video camera (MBF Biosciences, CX 9000). The live images of the sections of CN were analysed stereologically using the Stereo Investigator software (MicroBrightfield Inc. VT, USA). The Cavalieri probe was used to measure the entire volume of the CN. Subsequently, the optical fractionator was used for counting the total number of neurons and glia. Simultaneously with the fractionator, the nucleator probe was also applied in order to estimate the total volume and area of the neuronal profiles.

#### 2.2.1. Estimation of the cell population

Initially, a pilot study was undertaken to establish the study and sampling design.<sup>26–28</sup> Every 12th section of the sample

was selected and a grid size of  $300\ \mu\text{m} \times 300\ \mu\text{m}$  was applied. A counting frame of  $40\ \mu\text{m} \times 40\ \mu\text{m}$  with an optical dissector height of  $20\ \mu\text{m}$  and  $2\ \mu\text{m}$  guard zone was used to include 2–3 neurons within its limits. This procedure was adequate to include 100–150 neurons from one CN using 60X objective lens (oil) and also to obtain a coefficient of error (CE) of 0.05.<sup>29,30</sup>

To estimate the number of neurons and glia, optical fractionator was used along with the nucleator probe to measure the area and the total volume of the profiles. First, a contour was drawn around the region of interest at a low magnification objective lens ( $2\times$ ) and then using  $60\times$  objective lens (oil, NA 1.35), the optical fractionator and nucleator probes were initiated. The counting rule of first appearance of the profile across dissector height<sup>31</sup> and the ‘unbiased counting rule’ of Gundersen<sup>32</sup> and Sterio<sup>33</sup> {two exclusion edges (left and lower) and two inclusion edges (upper and right)} were used on the sections to count the number of neurons and glia.

The nucleator probe applied four isotropic rays from the marked centre of the nucleus. The intersection of these rays with the boundaries of the neuron and its nucleus were marked to generate the data of area and the total volume of the profiles. The data of neuronal and its nuclear volumes were used to assess the overall changes in their volume with aging. The data of neuron and its nuclear area were utilised for hierarchical cluster analysis.<sup>34</sup>

CE was calculated with the Gundersen–Jensen estimator<sup>35</sup> using smoothness constant ( $m$ ) of 1.

$$CE = \sqrt{\{[3(A - S^2) - 4B + C] \times \alpha' + S^2\} / Q^-}$$

where “A” is the sum of the squares of counts obtained from all individual sections of the sample; “B” is the sum of the products of the count in section  $i$  and subsequent section  $(i + 1)$  for all the sections of the sample; “C” is the sum of the products of the count in section  $i$  with the count in section  $i + 2$  for all the sections of the sample;  $S^2$  is the variance introduced by local errors for point counting;  $\alpha'$  is a value between  $1/12$  and  $1/240$  for smoothness factors of 0 and 1 and  $Q^-$  is the sum of the point or cell counts obtained in all sections of the sample.

The estimate of the total number of neurons and glia was calculated as<sup>22,31</sup>

$$N = \sum Q^- \times 1/\text{asf} \times 1/\text{ssf} \times t/h$$

where  $\sum Q^-$  is the total number of particles counted, “asf” is the area sampling fraction: counting frame area/grid size, “ssf” is the section sampling fraction: periodicity of sections, “t” is the mounted section thickness; “h” is the height of optical dissector.

### 2.2.2. Volume of the CN

To estimate the volume of the entire CN at various age groups, the Cavalieri probe was used. A contour was drawn around the region of interest. A pilot study estimated that the appropriate grid spacing was  $80\ \mu\text{m}$  to get an estimate of CE value of 0.05. After drawing the contour around the region of interest using  $2\times$  objective lens, the Cavalieri probe was applied using  $60\times$  objective lens. The grid points that lay within the contour of the region of interest were marked and

counted. The total volume (reference volume  $V_{\text{ref}}$ ) of the entire CN was estimated using the Cavalieri principle<sup>22</sup> as.

$$V(\text{ref}) = T \times \sum A$$

where  $T$  is the distance between each section and  $\sum A$  is the sum of the reference areas on the face of each section.

### 2.3. Statistical analysis

Statistical analysis was carried out using SPSS 20 version 20.0 (IBM Corp., 2011) software. Descriptive statistics such as mean and standard deviation were calculated. The data were tested for normality assumption using appropriate statistical test (Kolmogorov–Smirnov test). In the case of non-normal distribution, the nonparametric test (Kruskal–Wallis) followed by Dunnett's post-hoc test for multiple comparisons were used. Hierarchical cluster analysis was applied on neuron (NA) and neuronal nucleus area (NNA) (data derived from use of nucleator probe of the Stereo Investigator software) from decades one to nine in order to identify clusters that represents collection of data that are proximate based on a distance or dissimilarity function. An agglomerative (between-group linkage) method was applied using squared Euclidean distance interval measure, where clusters gradually merged in a way until each object fit into a cluster. The probable confounding variables such as age, gender and side of the brain (laterality) were taken into consideration while carrying out data analysis. However these variables were not found to be statistically significant for the present data. An overall ‘ $p$ ’ value of less than 0.05 was considered to be statistically significant. Statistical tests were not applied on the data of decade 9 specimens as there were only two samples.

## 3. Results

The brain weight for all cases studied ranged between 1250 and 1560 g except in the two- and twenty six day-old infants, where it was 370 g and 400 g, respectively. The CN, its subdivisions and various neurons were recognised as described previously.<sup>36</sup>

### 3.1. Stereological estimates

#### 3.1.1. Cell population

The mean values ( $\pm$ SD) of number of neurons and glia are given in Table 1. The minimum and maximum neuron number was observed in decades 1 and 3, respectively. The significant difference was found in the total number of neurons between decade 3 and decades 1, 2, 4, 6 and 7, respectively (decade 3 vs. decades 1, 2 and 6,  $p < 0.003$ ; decade 3 vs. decades 4 and 7,  $p < 0.03$ ; Table 1; Fig. 1). An increase in the total number of glia was noted in decade 9 but could not access statistically because of less sample size.

#### 3.1.2. Neuron, corresponding nucleus and CN volume

The mean values ( $\pm$ SD) of neuron, neuronal nucleus and entire CN volume are given in Table 1. The minimum and maximum neuronal volume, neuronal nuclear volume and

**Table 1 – Average ( $\pm$ SD) of human cochlear nucleus (CN) parameters using optical fractionator, nucleator and cavalieri probe.**

| Decade (years) | Total no of samples | Total no of neurons    | Total no of glia        | Neuronal volume ( $\mu\text{m}^3$ ) | Neuronal nucleus volume ( $\mu\text{m}^3$ ) | CN volume ( $\text{mm}^3$ ) |
|----------------|---------------------|------------------------|-------------------------|-------------------------------------|---|-----------------------------|
| Birth-10       | 4                   | 110,400 $\pm$ 15300**  | 2,151,000 $\pm$ 442,300 | 3700 $\pm$ 1000                     | 500 $\pm$ 130                               | 24 $\pm$ 2*                 |
| 11–20          | 5                   | 114,950 $\pm$ 16,800** | 1,482,000 $\pm$ 461,300 | 4100 $\pm$ 200                      | 600 $\pm$ 80                                | 27 $\pm$ 3                  |
| 21–30          | 5                   | 212,000 $\pm$ 15,100** | 1,633,000 $\pm$ 681,000 | 4800 $\pm$ 1300                     | 700 $\pm$ 40                                | 36 $\pm$ 7*                 |
| 31–40          | 5                   | 127,200 $\pm$ 34,500*  | 1,683,000 $\pm$ 429,100 | 4000 $\pm$ 800                      | 600 $\pm$ 120                               | 29 $\pm$ 5                  |
| 41–50          | 5                   | 139,000 $\pm$ 29,900   | 1,942,000 $\pm$ 468,500 | 4800 $\pm$ 1200                     | 600 $\pm$ 110                               | 32 $\pm$ 6                  |
| 51–60          | 5                   | 114,300 $\pm$ 54,100** | 1,966,000 $\pm$ 444,200 | 3800 $\pm$ 800                      | 500 $\pm$ 50                                | 25 $\pm$ 7                  |
| 61–70          | 5                   | 124,000 $\pm$ 41,300*  | 1,687,000 $\pm$ 487,500 | 4500 $\pm$ 600                      | 700 $\pm$ 120                               | 26 $\pm$ 3                  |
| 71–80          | 5                   | 140,200 $\pm$ 51,100   | 1,921,000 $\pm$ 443,500 | 4600 $\pm$ 1000                     | 700 $\pm$ 150                               | 30 $\pm$ 4                  |
| 81–90          | 2                   | 155,700 $\pm$ 30,500   | 2,999,000 $\pm$ 429,000 | 4200 $\pm$ 300                      | 600 $\pm$ 140                               | 25 $\pm$ 4                  |

\* $P < 0.05$ , \*\* $P < 0.005$  based on Kruskal–Wallis nonparametric test followed by Dunnett's post-hoc test for multiple comparisons with reference category decade 3.

entire CN volume was observed in decade 1 and decade 3 respectively. The entire CN volume in decade 3 was significantly higher as compared to decade 1 ( $p < 0.05$ ).

### 3.2. Cluster analysis

Based on agglomerative hierarchical cluster method, neurons were classified into different clusters using NA and NNA (Table 2, Fig. 2). The neuron clusters were arranged from smallest to largest size and the mean values of all the clusters were significantly different with each other ( $p < 0.001$ ). The maximum eight numbers of neuron clusters were identified in decades 2 and 3. The decades 1 and 4 had seven clusters and decades 5–8 had six clusters, respectively. The neurons of cluster 6 remained unchanged (9–10%) except, a marked reduction in the percentage was observed in decades 4 (2%) and 6 (1%). Neurons which belonged to cluster 8 were largest in size and their percentage remained unchanged (1–2%) in all the decades except in decades 2, 3 and 8, where it was 3–4% with NA/NNA ratio of  $4.0 \pm 1.1$  to  $4.8 \pm 1.9$  respectively.

In decade 1, the maximum percentage of neurons was seen in cluster 3 (35%, NA/NNA ratio  $3.9 \pm 1.0$ ), whereas in decades 2 and 3, maximum percentage of neurons was noted in clusters 2 and 1 (24%, NA/NNA ratio  $3.6 \pm 1.9$  and 37%, NA/NNA ratio  $4.5 \pm 2.2$  respectively). The neurons in cluster 5 were only observed in decades 2 (8%) and 3 (3%) with the corresponding NA/NNA ratios of  $6.0 \pm 0.01$  and  $3.3 \pm 0.9$  respectively.

In decade 4, the percentage of neurons was maximum in clusters 1 and 2 (40%, NA/NNA ratio of  $3.0 \pm 1.6$  and  $3.4 \pm 1.7$  respectively). Due to changes in the NA/NNA of neurons of cluster 5, there was a likelihood of merging of neurons of cluster 5 with cluster 4 as an increase in the percentage of small size neurons was observed as compared to the larger size neurons [as depicted with dark red colour diamond ( $\blacklozenge$ ) in Fig. 2 from D 4 – D 8]. Further remarkable reduction in the percentage of neurons of clusters 4, 6 and 7 was observed. In decade 5, the maximum percentage of neurons was seen in cluster 2 (38%, NA/NNA ratio of  $3.4 \pm 1.0$ ). Changes in NA/NNA distribution were observed and neurons of cluster 3 were merged with cluster 2 (as depicted with fluorescent green colour triangle ( $\blacktriangle$ ), Fig. 2) till decade 8.

In decades 6 and 7, the maximum percentage of neurons belonged to clusters 1 and 4 (40% and 37%) was seen (NA/NNA

ratio of  $3.4 \pm 1.7$  and  $3.9 \pm 2.3$  respectively). In decade 8, the maximum percentage of neurons of cluster 2 was seen (35%, NA/NNA ratio of  $3.7 \pm 1.2$ ). In decade 9, only four clusters (1, 4, 7 and 8) were observed and further statistical interpretation was within the limit of small sample size.

## 4. Discussion

To the best of our knowledge, this is the first stereological study of the age related changes in the human CN, ranging from birth to 90 years of age. We observed that among all age groups studied, decade 1 had minimum and 3 had maximum nuclear volume and neuron number respectively. The mean neuron and neuron nucleus volume was also increased during this period. There was an increase in total glial population in decade 9. Different neuron clusters were identified and changes were observed within the clusters over the decades.

There are contradictory reports regarding the age related morphological changes in the CN in animal species and humans. A decrease in the volume, neuronal number and neuron size of the CN and preference for particular type of neurons have been reported in animal models of age related hearing loss.<sup>12,14,37,38</sup> The qualitative and quantitative studies on human CN showed variable results with unremarkable changes and/or cell loss.<sup>16,17</sup> A higher range of number of glial cells and neurons, in the volume of neurons and the corresponding nucleus and in the entire CN was noted in the present study in comparison to the earlier reports.<sup>9,14,17</sup> This discrepancy may be because the previous studies on human CN neither included a large sample size representing all the decades nor used unbiased stereology as a method of quantification.<sup>22,31</sup> The reported mean neuron population in the entire adult human CN was 91,470<sup>17</sup> and 97,000 (without granule cell counts)<sup>9</sup> whereas in VCN it was reported to be 63,200.<sup>14</sup> A significant increase in the mean CN neuronal population was observed in the presbycusis group (114,170).<sup>17</sup> Our study included brainstems from 2 days to 90 years of age that covered a complete spectrum of different ages and the minimum and maximum neuronal number was observed in decade 1 and 3 respectively. Predominantly the small cells may be contributing to this increase in neuronal number in decade 3 as observed in our cluster analysis and also reported

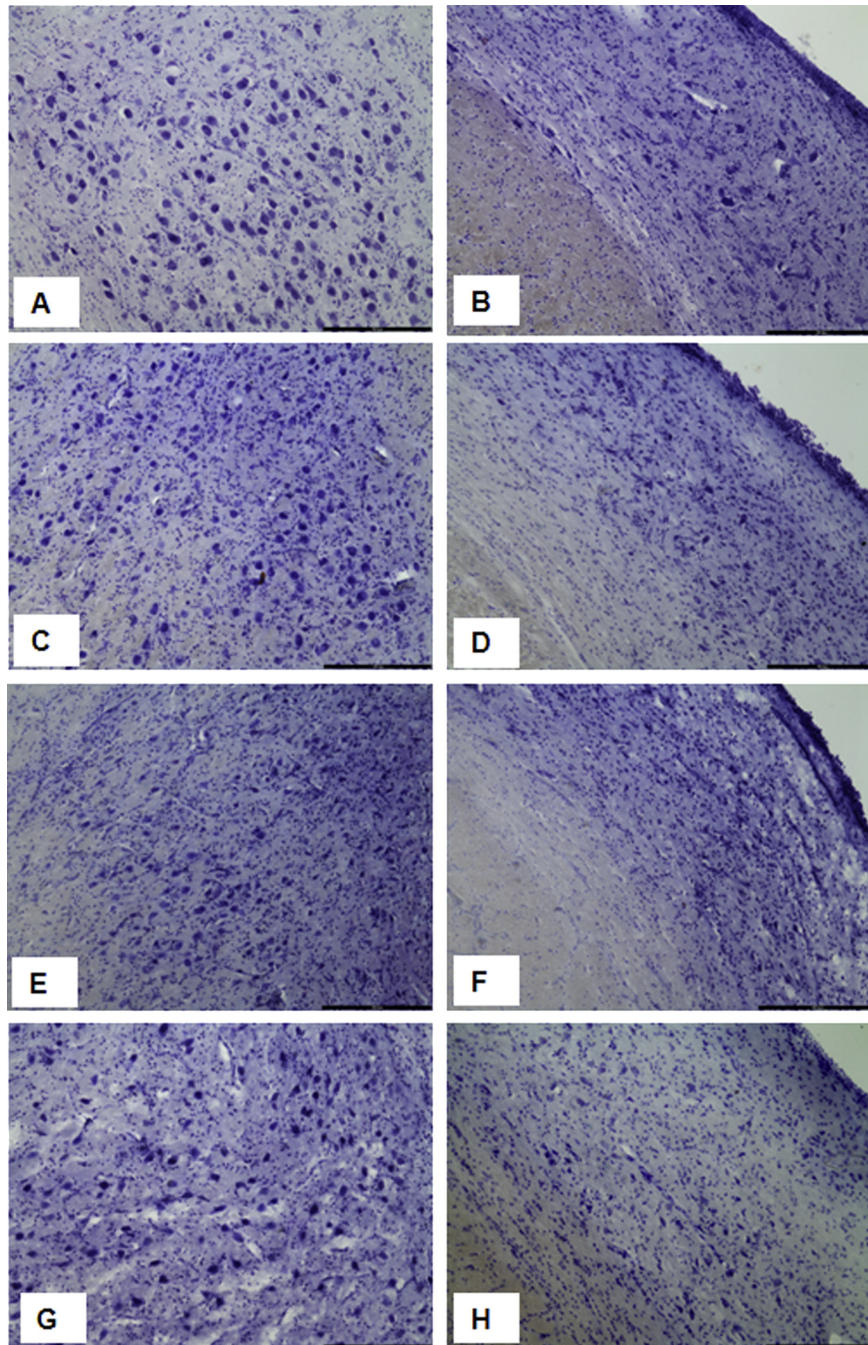


**Fig. 1** – Representative photomicrographs of Nissl stained transverse sections of two subdivisions of human cochlear nucleus (CN). (A–B) VCN and DCN in decade 1 (3 years), (C–D) VCN and DCN in decade 3 (30 years), (E–F) VCN and DCN in decade 6 (60 years), (G–H) VCN and DCN in decade 7 (70 years). The significant difference was found in the total number of neurons between decade 3 and decades 1, 6 and 7, respectively (decade 3 vs. decades 1 and 6,  $p < 0.003$ ; decade 3 vs. decade 7,  $p < 0.03$ . Scale bars: 300  $\mu\text{m}$ .

in rat trigeminal ganglion due to maturation of dormant, post-mitotic precursors.<sup>39</sup> A decrease in human CN volume was also reported between 50 and 90 years of age.<sup>14</sup> In our study the mean CN volume was significantly increased in decade 3 which may be due to initial proliferation of the neuronal processes (dendrites and axons) followed by pruning and/or plastic changes. None of the previous studies have reported

glial cell population counts with progressive age. There are few immunohistochemical studies showing increase in glial fibrillary acidic protein (GFAP) immunoreactivity in astrocytes in the rat and human CN with aging.<sup>18,19</sup> In our study, decade 9 had shown two folds increase in total glial cells. We have also observed a significant increase in GFAP immunoreactivity in decades 5–8 respectively.<sup>19</sup> This increase in glial number may

**Table 2 – Distribution of neurons (%) and descriptive measures (mean  $\pm$  SD) of neuron area (NA), neuron nucleus area (NNA) and NA/NNA ratio by cluster and decade.**

| Distribution of percentage of neurons (%), neuron area (NA), neuron nucleus area (NNA) and NA/NNA ratio in each cluster with decade |                         |                  |                  |                  |                  |                  |                  |                   |                  |
|---|-------------------------|------------------|------------------|------------------|------------------|------------------|------------------|-------------------|------------------|
| Decade  | Parameters              | Cluster 1        | Cluster 2        | Cluster 3        | Cluster 4        | Cluster 5        | Cluster 6        | Cluster 7         | Cluster 8        |
| 1   | %                       | 13.8             | 20.0             | 35.4             | 16.9             | *                | 9.2              | 3.1               | 1.5              |
|   | NA ( $\mu\text{m}^2$ )  | 102.9 $\pm$ 22.8 | 188.4 $\pm$ 26.9 | 287.8 $\pm$ 34.9 | 384.4 $\pm$ 29.6 | *                | 536.4 $\pm$ 30.1 | 645.3 $\pm$ 12.6  | 716.9 $\pm$ 7.0  |
|   | NNA ( $\mu\text{m}^2$ ) | 22.3 $\pm$ 9.8   | 53.0 $\pm$ 5.6   | 78.1 $\pm$ 19.9  | 116.5 $\pm$ 17.0 | *                | 131.1 $\pm$ 26.0 | 184.2 $\pm$ 29.2  | 212.9 $\pm$ 7.0  |
| 2   | NA/NNA                  | 5.1 $\pm$ 1.5    | 3.5 $\pm$ 0.6    | 3.9 $\pm$ 1.0    | 3.3 $\pm$ 0.65   | *                | 4.2 $\pm$ 0.8    | 3.5 $\pm$ 0.6     | 3.3 $\pm$ 0.07   |
|   | %                       | 16.6             | 24.0             | 9.7              | 13.7             | 8.6              | 9.1              | 14.3              | 4.0              |
|   | NA ( $\mu\text{m}^2$ )  | 127.3 $\pm$ 31.8 | 209.5 $\pm$ 25.9 | 294.4 $\pm$ 15.8 | 271.7 $\pm$ 21.3 | 359.8 $\pm$ 20.7 | 327.6 $\pm$ 31.0 | 465.8 $\pm$ 43.1  | 547.9 $\pm$ 50.8 |
| 3   | NNA ( $\mu\text{m}^2$ ) | 51.7 $\pm$ 19.9  | 71.5 $\pm$ 27.7  | 53.7 $\pm$ 13.4  | 97.2 $\pm$ 14.2  | 64.6 $\pm$ 17.2  | 118.7 $\pm$ 24.4 | 78.8 $\pm$ 23.8   | 124.0 $\pm$ 30.7 |
|   | NA/NNA                  | 2.9 $\pm$ 1.8    | 3.6 $\pm$ 1.9    | 5.9 $\pm$ 2.04   | 2.8 $\pm$ 0.4    | 6 $\pm$ 2.03     | 2.9 $\pm$ 0.9    | 6.5 $\pm$ 2.5     | 4.8 $\pm$ 1.9    |
|   | %                       | 37.9             | 11.7             | 16.5             | 11.7             | 3.9              | 9.7              | 4.9               | 3.9              |
| 4   | NA ( $\mu\text{m}^2$ )  | 136.7 $\pm$ 30.2 | 229.6 $\pm$ 19.0 | 293.0 $\pm$ 14.3 | 352.4 $\pm$ 18.6 | 412.8 $\pm$ 7.5  | 489.6 $\pm$ 19.8 | 560.2 $\pm$ 15.8  | 650.5 $\pm$ 65.6 |
|   | NNA ( $\mu\text{m}^2$ ) | 35.3 $\pm$ 14.1  | 74.3 $\pm$ 23.2  | 87.4 $\pm$ 18.8  | 102.4 $\pm$ 28.0 | 134.1 $\pm$ 43.2 | 133.9 $\pm$ 18.8 | 146.4 $\pm$ 19.5  | 167.5 $\pm$ 38.0 |
|   | NA/NNA                  | 4.5 $\pm$ 2.2    | 3.3 $\pm$ 1.0    | 3.4 $\pm$ 0.7    | 3.6 $\pm$ 0.88   | 3.3 $\pm$ 0.9    | 3.7 $\pm$ 0.5    | 3.9 $\pm$ 0.6     | 4.0 $\pm$ 1.1    |
| 5   | %                       | 40.2             | 23.3             | 27.5             | 5.3              | *                | 2.1              | 0.5               | 1.1              |
|   | NA ( $\mu\text{m}^2$ )  | 149.9 $\pm$ 38.0 | 256.0 $\pm$ 28.8 | 372.4 $\pm$ 37.5 | 484.7 $\pm$ 28.6 | *                | 557.1 $\pm$ 46.4 | 623.8 $\pm$ 39.3  | 783.4 $\pm$ 49.3 |
|   | NNA ( $\mu\text{m}^2$ ) | 57.0 $\pm$ 21.1  | 81.83 $\pm$ 22.2 | 118.2 $\pm$ 37.3 | 107.4 $\pm$ 10.0 | *                | 196.2 $\pm$ 21.0 | 109.6 $\pm$ 14.0  | 133.3 $\pm$ 18.0 |
| 6   | NA/NNA                  | 3 $\pm$ 1.6      | 3.4 $\pm$ 1.2    | 3.5 $\pm$ 1.5    | 4.5 $\pm$ 0.4    | *                | 2.8 $\pm$ 0.2    | 5.6 $\pm$ 0.1     | 5.8 $\pm$ 0.1    |
|   | %                       | 22.4             | 38.3             | *                | 24.0             | *                | 9.3              | 4.4               | 1.6              |
|   | NA ( $\mu\text{m}^2$ )  | 149.1 $\pm$ 31.8 | 281.3 $\pm$ 46.9 | *                | 462.6 $\pm$ 48.6 | *                | 612.4 $\pm$ 32.8 | 715.0 $\pm$ 33.8  | 864.2 $\pm$ 21.9 |
| 7   | NNA ( $\mu\text{m}^2$ ) | 49.8 $\pm$ 18.1  | 88.0 $\pm$ 27.6  | *                | 121.6 $\pm$ 36.6 | *                | 137.7 $\pm$ 41.7 | 193.5 $\pm$ 55.7  | 229.3 $\pm$ 42.1 |
|   | NA/NNA                  | 3.4 $\pm$ 1.6    | 3.4 $\pm$ 1.1    | *                | 4.2 $\pm$ 1.5    | *                | 4.9 $\pm$ 1.6    | 3.9 $\pm$ 1.2     | 3.9 $\pm$ 0.1    |
|   | %                       | 40.0             | 30.5             | *                | 22.4             | *                | 1.4              | 4.3               | 1.4              |
| 8   | NA ( $\mu\text{m}^2$ )  | 165.5 $\pm$ 48.5 | 313.8 $\pm$ 39.3 | *                | 462.5 $\pm$ 42.0 | *                | 586.4 $\pm$ 31.8 | 616.4 $\pm$ 39.5  | 735.5 $\pm$ 12.1 |
|   | NNA ( $\mu\text{m}^2$ ) | 56.4 $\pm$ 22.6  | 95.2 $\pm$ 28.5  | *                | 111.5 $\pm$ 34.3 | *                | 194.6 $\pm$ 22.0 | 107.1 $\pm$ 22.5  | 216.1 $\pm$ 71.9 |
|   | NA/NNA                  | 3.4 $\pm$ 1.7    | 3.6 $\pm$ 1.1    | *                | 4.5 $\pm$ 1.4    | *                | 3 $\pm$ 0.4      | 6 $\pm$ 1.3       | 3.6 $\pm$ 1.1    |
| 9   | %                       | 28.8             | 22.7             | *                | 36.4             | *                | 6.1              | 5.1               | 1.0              |
|   | NA ( $\mu\text{m}^2$ )  | 140.3 $\pm$ 33.1 | 256.2 $\pm$ 31.6 | *                | 378.3 $\pm$ 48.7 | *                | 523.2 $\pm$ 24.6 | 620.0 $\pm$ 31.0  | 817.1 $\pm$ 24.7 |
|   | NNA ( $\mu\text{m}^2$ ) | 45.9 $\pm$ 19.9  | 76.2 $\pm$ 24.9  | *                | 111.3 $\pm$ 33.8 | *                | 150.2 $\pm$ 35.2 | 143.6 $\pm$ 56.8  | 141.8 $\pm$ 37.7 |
| 10  | NA/NNA                  | 3.5 $\pm$ 1.7    | 3.8 $\pm$ 1.5    | *                | 3.9 $\pm$ 2.3    | *                | 3.6 $\pm$ 0.8    | 4.8 $\pm$ 1.4     | 5.9 $\pm$ 1.4    |
|   | %                       | 28.1             | 35.6             | *                | 12.7             | *                | 12.7             | 7.1               | 3.7              |
|   | NA ( $\mu\text{m}^2$ )  | 144.9 $\pm$ 35.0 | 254.5 $\pm$ 39.5 | *                | 359.8 $\pm$ 24.9 | *                | 440.2 $\pm$ 26.5 | 559.7 $\pm$ 43.5  | 727.3 $\pm$ 72.2 |
| 11  | NNA ( $\mu\text{m}^2$ ) | 54.8 $\pm$ 19.9  | 72.9 $\pm$ 19.9  | *                | 113.2 $\pm$ 19.3 | *                | 95.3 $\pm$ 28.9  | 123.46 $\pm$ 43.4 | 156.8 $\pm$ 32.2 |
|   | NA/NNA                  | 2.9 $\pm$ 1.0    | 3.7 $\pm$ 1.2    | *                | 3.2 $\pm$ 0.5    | *                | 5.0 $\pm$ 1.4    | 4.9 $\pm$ 1.4     | 4.7 $\pm$ 0.8    |
|   | %                       | 40.9             | *                | *                | 47.2             | *                | *                | 11.4              | 0.5              |
| 12  | NA ( $\mu\text{m}^2$ )  | 155.6 $\pm$ 48.5 | *                | *                | 324.4 $\pm$ 54.2 | *                | *                | 528.7 $\pm$ 62.1  | 920.3            |
|   | NNA ( $\mu\text{m}^2$ ) | 50.2 $\pm$ 22.5  | *                | *                | 79.0 $\pm$ 32.9  | *                | *                | 107.3 $\pm$ 33.3  | 124.3            |
|   | NA/NNA                  | 3.7 $\pm$ 2.5    | *                | *                | 4.8 $\pm$ 2.1    | *                | *                | 5.4 $\pm$ 1.9     | 7.4              |

\*Indicates that because of different values of NA/NNA, the similar number of clusters (8) were not identified except in decade 2 and 3.

be an astrocytic reaction to intrinsic modifications in the CN such as degeneration of neighbouring synapses, dendrites or entire neurons as observed in the aging CN.<sup>40,41</sup>

Cluster analysis is an exploratory data analysis to discover a system of organizing observations, into groups, where members of the groups share properties in common tool. In the earlier studies<sup>7-9</sup> it was observed that there is different neuron populations in the CN based on their sizes. Decade 1 had seven clusters and the maximum number of neurons was found in cluster 3. According to neuron area, cluster 3 neurons could be categorised as fusiform neurons of the DCN which is responsible for high frequency information processing and participate in the complex intrinsic circuit in the DCN.<sup>7,9,10</sup> As reported, studies on human foetus have shown relatively good transmission of low frequencies as compared to higher frequencies,<sup>42</sup> the presence of maximum number of cluster 3 neurons may suggest the development of high frequency information processing and intrinsic circuitry take place in the DCN during decade 1.

In decades 2 and 3, two major changes were observed. Firstly, the maximum number of neurons shifted from cluster 3 to clusters 2 and then to cluster 1. Based on their size<sup>7,17</sup> cluster 1 and 2 neurons could be categorised into granule and small cells, which were found caudo-rostrally from dorsal cochlear nucleus (DCN) to lateral part of the VCN.<sup>7,17</sup> The granule cells receive non-auditory inputs and integrate a wide spectrum of information carrying cues about attention, head position, sound localization, or recognition and further may influence the function and output of the DCN.<sup>43-45</sup> Secondly, a discrete cluster of neurons (cluster 5) was identified and according to their neuron area they could be categorised as octopus neurons.<sup>7,17</sup> There is a considerable literature on the potential risk to hearing from various types of social noise exposure especially during decade 2 and 3<sup>46</sup> which could contribute to these changes within these neurons clusters.

In decade 4, due to changes in the NA/NNA, the cluster 5 neurons formed a common group [(♦) dark red colour in Fig. 2 from D 4 – D 8] with cluster 4 neurons. Further remarkable

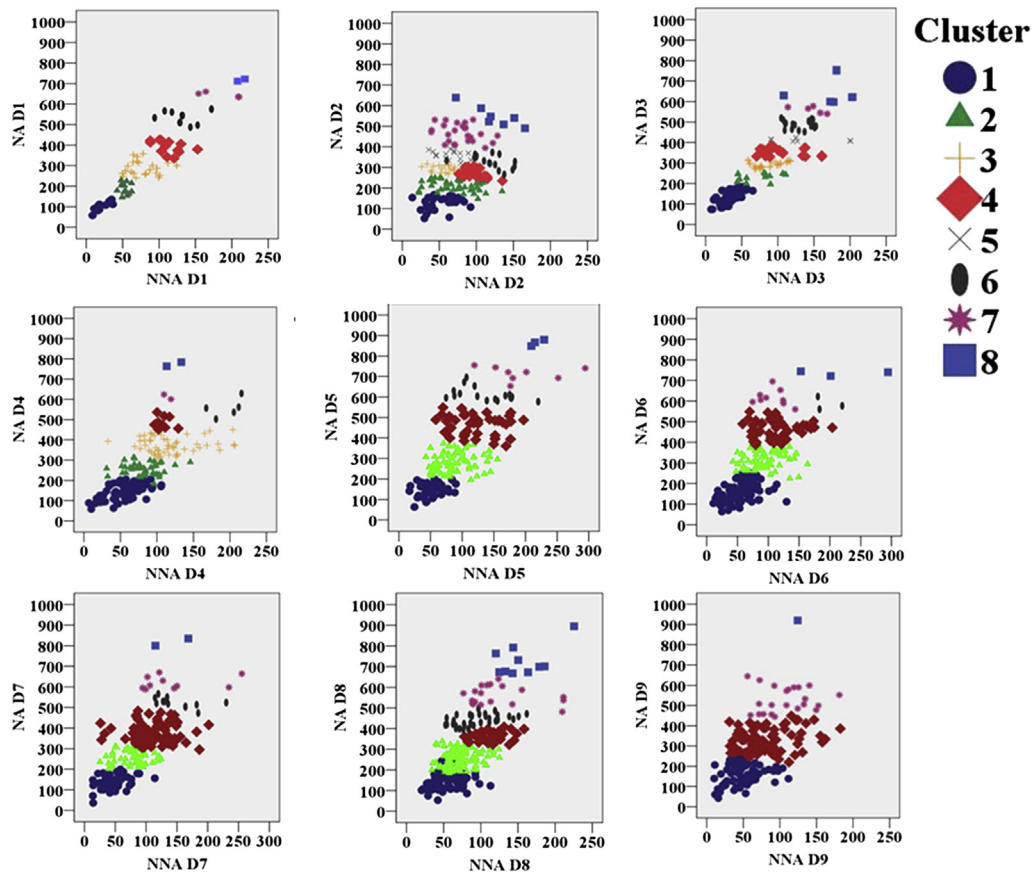


**Fig. 2** – The scatter plot illustrates arrangement of neuron clusters (1–8) and their changes in decades 1–9, using different coloured symbols, identified by the agglomerative hierarchical cluster algorithm applied on data of neuron area (NA) and neuron nucleus area (NNA) in human CN. X and Y axis represents NA and NNA, D1-D 9 represent the decades 1–9.

reduction in clusters 4, 6 and 7 neurons was observed. These 4, 6 and 7 clusters could be categorised as multipolar, spherical and globular bushy neurons<sup>7,17</sup> according to their area. This reduction in the percentage of large size neurons in decade 4 may be because of noise exposure of low sound intensities in the older children and adulthood results in temporary alterations in hearing with a limited threshold shift and recovery of hearing sensitivity after some time<sup>46</sup> which needs to investigate further using functional studies.

Within decades 5–8, major changes happened in NA/NNA of cluster 3 neurons and this neuron cluster form a common group with cluster 2. As cluster 3 neurons could be classified as fusiform cells,<sup>7,17</sup> which are responsible for high frequency information processing.<sup>10</sup> These changes may be suggestive of beginning of loss of high frequencies<sup>47</sup> and further may affect the complex intrinsic circuit in the DCN indicate plastic changes in the restricted group of DCN neurons.<sup>48</sup>

## 5. Conclusion

We observed that there is no uniformity within the age related changes among different neuronal groups. With aging, a majority of the human CN neurons undergo morphological changes, but the small to medium sized neurons are affected

more than the large sized, especially after the decade 5, as revealed from our study. It indicates that the eight neuron clusters show changes within themselves and they raise the possibility of some compensatory mechanism and/or plastic response within the CN neurons without much alteration in various morphometric parameters with age. Therefore, further studies are needed to integrate the results of anatomical, physiological, neurochemical and behavioural studies before we understand fully how these diverse and specialized cells undergo morphological changes and consequently contribute to the complex functioning of the CN with advancing age. The results of the present study may add new insight in understanding the pathophysiology of hearing loss with age.

## Funding source

This work was supported by funds from Indian Council of Medical Research, New Delhi (5/8/10-2(oto)/2009-NCD-1).

## Conflicts of interest

All authors have none to declare.

## Acknowledgements

We acknowledge the contribution of Prof. Alok Thakar from department of Otorhinolaryngology and the faculty and residents of the department of Forensic Medicine and Toxicology. This work was presented as poster (353.05) in the 43rd meeting of the Society for Neuroscience 2013, San Diego, USA.

## REFERENCES

- Howarth A, Shone GR. Ageing and the auditory system. *Postgrad Med J.* 2006;82:66–171.
- Gates GA, Rees TS. Hear ye? Hear ye! Successful auditory aging. *West J Med.* 1997;167:247–252.
- Weinstein BE, Ventry IM. Hearing impairment and social isolation in the elderly. *J Speech Hear Res.* 1982;25:593–599.
- Gordon-Salant S, Fitzgibbons PJ. Temporal factors and speech recognition performance in young and elderly listeners. *J Speech Hear Res.* 1993;36:1276–1285.
- Frisina DR, Frisina RD. Speech recognition in noise and presbycusis: relations to possible neural mechanisms. *Hear Res.* 1997;106:95–104.
- Woods DL, Clayworth CC. Age-related changes in human middle latency auditory evoked potentials. *Electroencephalogr Clin Neurophysiol.* 1986;65:297–303.
- Moore JK, Osen KK. The cochlear nuclei in man. *Am J Anat.* 1979;154:393–418.
- Adams JC. Neuronal morphology in the human cochlear nucleus. *Arch Otolaryngol.* 1986;112:1253–1261.
- Wagoner JL, Kulesza RJ. Topographical and cellular distribution of perineuronal nets in the human cochlear nucleus. *Hear Res.* 2009;254:42–53.
- Ryugo DK, Parks TN. Primary innervation of the avian and mammalian cochlear nucleus. *Brain Res Bull.* 2003;60:435–456.
- Willott JF, Bross LS, McFadden SL. Morphology of the dorsal cochlear nucleus in C57BL/6J and CBA/J mice across the life span. *J Comp Neurol.* 1992;321:666–678.
- Willott JF, Bross LS. Morphological changes in the anteroventral cochlear nucleus that accompany sensorineural hearing loss in DBA/2J and C57BL/6J mice. *Brain Res Dev Brain Res.* 1996;9:218–226.
- Bao J, Ohlemiller KK. Age-related loss of spiral ganglion neurons. *Hear Res.* 2010;264:93–97.
- Konigsmark BW, Murphy EA. Volume of the cochlear nucleus in man: its relationship to neuronal population and age. *J Neuropathol Exp Neurol.* 1972;31:304–316.
- Gandolfi A, Horoupian DS, DeTeresa RM. Quantitative and cytometric analysis of the ventral cochlear nucleus in man. *J Neurol Sci.* 1981;50:443–455.
- Arnesen AR. Presbycusis – Loss of neurons in the human cochlear nuclei. *J Laryngol Otol.* 1982;96:503–511.
- Hinojosa R, Nelson EG. Cochlear nucleus neuron analysis in individuals with presbycusis. *Laryngoscope.* 2011;121:2641–2648.
- Jalenques I, Albuissou E, Despres G, Romand R. Distribution of glial fibrillary acidic protein (GFAP) in the cochlear nucleus of adult and aged rats. *Brain Res.* 1995;686:223–232.
- Sharma S, Nag TC, Thakar A, Bhardwaj DN, Roy TS. The aging human cochlear nucleus: changes in the glial fibrillary acidic proteins, intracellular calcium regulatory proteins, GABAergic neurotransmitter and cholinergic receptors. *J Chem Neuroanat.* 2014;56:1–12.
- Montgomery DL. Astrocytes: forms, functions and role in disease. *Vet Pathol.* 1994;31:145–167.
- Gehrmann J, Matsumoto Y, Kreutzberg GW. Microglia: intrinsic immune effector cell of the brain. *Brain Res Brain Res Rev.* 1995;20:269–287.
- Howard CV, Reed MG. *Unbiased Stereology: Three Dimensional Measurement in Microscopy.* New York: Springer-Verlag; 1998.
- Ray B, Roy TS, Wadhwa S, Roy KK. Development of the human fetal cochlear nerve: a morphometric study. *Hear Res.* 2005;202:74–86.
- Sharma V, Nag TC, Wadhwa S, Roy TS. Stereological investigation and expression of calcium-binding proteins in developing human inferior colliculus. *J Chem Neuroanat.* 2009;37:78–86.
- Peinado MA, Quesada A, Pedrosa JA, et al. Light microscopic quantification of morphological changes during aging in neurons and glia of the rat parietal cortex. *Anat Rec.* 1997;247:420–425.
- West MJ, Østergaard K, Andreassen OA, Finsen B. Estimation of the number of somatostatin neurons in the striatum: an in situ hybridization study using the optical fractionator method. *J Comp Neurol.* 1996;370:11–22.
- Schmitz C, Hof PR. Design-based stereology in neuroscience. *Neuroscience.* 2005;130:813–831.
- Glaser JR, Greene G, Hendricks S. *Stereology for Biological Research.* Williston, VT: M.B.F. Press; 2007.
- Gundersen HJG, Østerby R. Optimizing sampling efficiency of stereological studies in biology: or 'do more less well!'. *J Microsc.* 1981;121:65–73.
- Schmitz C. Variation of fractionator estimates and its prediction. *Anat Embryol.* 1998;198:371–397.
- West MJ, Slomianka L, Gundersen HJ. Unbiased stereological estimation of the total number of neurons in the subdivisions of the rat hippocampus using optical fractionator. *Anat Rec.* 1991;231:482–497.
- Gundersen HJG. Notes on estimation of numerical density of arbitrary profiles: the edge effect. *J Microsc.* 1977;111:219–223.
- Sterio DC. The unbiased estimation of number and sizes of arbitrary particles using the disector. *J Microsc.* 1984;134:127–136.
- Potrusil T, Wenger C, Glueckert R, Schrott-fischer A, Rattay F. Morphometric classification and spatial organization of spiral ganglion neurons in the human cochlea: consequences for single fiber response to electrical stimulation. *Neuroscience.* 2012;214:120–135.
- Gundersen HJG, Jensen EB, Kieu K, Nielsen J. The efficiency of systematic sampling in stereology-reconsidered. *J Microsc.* 1999;193:199–211.
- Sharma S, Nag TC, Thakar A, et al. Age associated changes in the human cochlear nucleus - a three-dimensional modelling and its potential application for brainstem implants. *J Anat Soc India.* 2014;63:12–18.
- Frisina RD, Walton JP. Age-related structural and functional changes in the cochlear nucleus. *Hear Res.* 2006;216–217:216–223.
- Hansen CC, Reske-Nielsen E. Pathological studies in presbycusis: cochlear and central findings in 12 aged patients. *Arch Otolaryngol.* 1965;82:115–132.
- Lagares A, Li HY, Zhou XF, Avendano C. Primary sensory neuron addition in the adult rat trigeminal ganglion: evidence for neural crest glio-neuronal precursor maturation. *J Neurosci.* 2007;27:7939–7953.
- Geinisman Y, Bondareff W, Dodge JT. Hypertrophy of astroglial processes in the dentate gyrus of the senescent rat. *Am J Anat.* 1978;153:537–543.
- Adams I, Jones DG. Synaptic remodelling and astrocytic hypertrophy in rat cerebral cortex from early to late adulthood. *Neurobiol Aging.* 1982;3:179–186.
- Bench J. Sound transmission to the human foetus through the maternal abdominal wall. *J Genet Psychol.* 1968;113:85–87.

43. Itoh K, Kamiya H, Mitani A, Yasui Y, Takada M, Mizuno N. Direct projections from the dorsal column nuclei and the spinal trigeminal nuclei to the cochlear nuclei in the cat. *Brain Res.* 1987;400:145–150.
44. Weinberg RJ, Rustioni A. A cuneocochlear pathway in the rat. *Neuroscience.* 1987;20:209–219.
45. Weedman DL, Pongstaporn T, Ryugo DK. Ultrastructural study of the granule cell domain of the cochlear nucleus in rats: mossy fiber endings and their targets. *J Comp Neurol.* 1996;369:345–360.
46. Passchier-Vermeer W, Passchier WF. Noise exposure and public health. *Environ Health Perspect.* 2000;108:123–131.
47. Era P, Jokela J, Qvarnberg Y, Heikkinen E. Pure-tone thresholds, speech understanding and their correlates in samples of men of different ages. *Audiology.* 1986;25:338–352.
48. Shore SE. Plasticity of somatosensory inputs to the cochlear nucleus – implications for tinnitus. *Hear Res.* 2011;281:38–46.